guide wires. However, the development of guide wires suited for interventional MRI is warranted.

Preoperatively, MRI allowed noninvasive assessment of cardiovascular anatomy and function. During and after implantation, the position of the prosthetic valve was easy to determine. Besides this morphologic information, MRI provided immediate post-intervention physiologic parameters of cardiac function and perfusion of the proximal course of the coronary arteries. In addition, VEC MRI demonstrated optimal function of the implanted prosthetic valve in five cases and mild central valvular insufficiency in two cases.

In conclusion, the results of this study imply that MRI is a promising tool for transcatheter placement of valved stents. However, further validation of safety aspects is needed in chronic studies with larger numbers of animals.

*Titus Kuehne, MD
Sevim Yilmaz, MD
Carolin Meinus, MD
Phillip Moore, MD
Maythem Saeed, DVM, PhD
Oliver Weber, PhD
Charles B. Higgins, MD
Thiemo Blank, PhD
Erhard Elsaesser

Bernhard Schnackenburg, PhD
Peter Ewert, MD
Peter E. Lange, MD
Eike Nagel, MD

*Department of Congenital Heart Diseases
  and Pediatric Cardiology
German Heart Institute
Augustenburger Platz 1
Berlin, 13553
Germany
E-mail: titus.kuehne@dhzb.de

REFERENCES

1. Boudjemline Y, Bonhoeffer P. Steps toward percutaneous aortic valve replacement. Circulation 2002;105:775–8.
2. Cribier A, Eltchaninoff H, Bash A, et al. Percutaneous transcatheter implantation of an aortic valve prosthesis for calcific aortic stenosis: first human case description. Circulation 2002;106:3006–8.
3. Kuehne T, Saeed M, Higgins CB, et al. Endovascular stents in pulmonary valve and artery in swine: feasibility study of MR imaging-guided deployment and postinterventional assessment. Radiology 2003;226:475–81.

Feasibility of Adjusting Paced Left Ventricular Activation by Manipulating Stimulus Strength

To the Editor: Cardiac resynchronization therapy (CRT) improves symptoms and decreases hospitalizations in selected patients with heart failure (1,2). With CRT, pacing from the left ventricle (LV) alters the ventricular activation (VA) sequence, changing the QRS morphology. In responders, change in VA improves cardiac filling and ejection (3). However, many patients are nonresponders. The LV lead location is the major determinant of paced activation but is often constrained by the location of coronary sinus vein branches. During LV mapping for ventricular tachycardia, increased pacing stimulus strength (SS) has been demonstrated to capture an enlarged myocardial area, producing a larger "virtual electrode" (4). If the enlarged area of myocardial capture extends beyond a discrete region of conduction block, the SS increase could result in VA change and more rapid conduction to a remote location, such as the right ventricular (RV) apex.

We hypothesized that paced VA can be manipulated by increasing SS. We expected activation changes to be more marked when pacing near areas of scarred or infarcted myocardium.

Ten patients with New York Heart Association functional class II and III congestive heart failure, ejection fraction <40%, referred for ablation were enrolled according to protocols approved by the Brigham and Women's Hospital human subject protection committee.

Using an electroanatomic mapping system (CARTO, Biosense-Webster Inc., Diamond Bar, California), three-dimensional plots (mean of 136 ± 47 points per patient) of bipolar electrogram amplitude were created (5). Endocardial LV mapping was performed with a 7-F steerable catheter (Biosense-Webster Inc.). Electrograms were recorded on a separate digital system (Prucka Engineering Inc., Houston, Texas). Epicardial mapping by percutaneous subxiphoid approach was performed in one patient. Catheter stability was confirmed by biplane fluoroscopy, the mapping system, and continuous monitoring of electrogram morphology and timing.

Pacing at outputs of threshold, 5 mA, and 10 mA was performed at 6 to 10 separated LV sites. In one case, epicardial pacing at 20 mA was performed because of high pacing threshold (10 mA). The anode was in the inferior vena cava (IVC). A quadripolar catheter at the RV apex was the reference catheter. Atrial, ventricular, and His bundle electrograms were assessed to exclude antegrade atrial conduction during pacing.

Stimulus to RV conduction times and stimulus to QRS conduction times (QRS latency) were measured from the stimulus artifact to the first bipolar peak of the electrogram from the RV apical catheter and to the earliest VA in the surface electrocardiogram (ECG). Changes in QRS morphology with pacing were defined as any of the following: QRS width change of >40 ms; new Q-, R-, or S-wave of >25% of the total QRS amplitude; >50% change in ratio of R or S components of QRS complex;

Table 1. Parameters With Stimulus Strength Alteration

	Total	Unchanged QRS	Changed QRS	p Value†
Pacing sites	95	78	17	
Stim to RV (ms)				
Threshold	118 ± 62*	111 ± 52*	150 ± 93	<0.0001
10 mA	95 ± 43	96 ± 43	87 ± 44	
QRS duration (ms)				
Threshold	199 ± 39*	196 ± 40‡	213 ± 28‡	0.03
10 mA	192 ± 43	191 ± 37	195 ± 31	
QRS latency (ms)				
Threshold	47 ± 52*	36 ± 39‡	99 ± 73‡	<0.0001
10 mA	32 ± 34	27 ± 29	54 ± 49	
Electrogram amplitude (mV)	2.0 ± 2.0	2.3 ± 2.1	0.8 ± 1.1	0.007

*$p < 0.001$ for comparison of threshold with 10 mA stimulus strengths. †p value reported for changed versus unchanged QRS. ‡$p \leq 0.05$ for threshold versus 10 mA stimulus strengths.
RV = right ventricle.
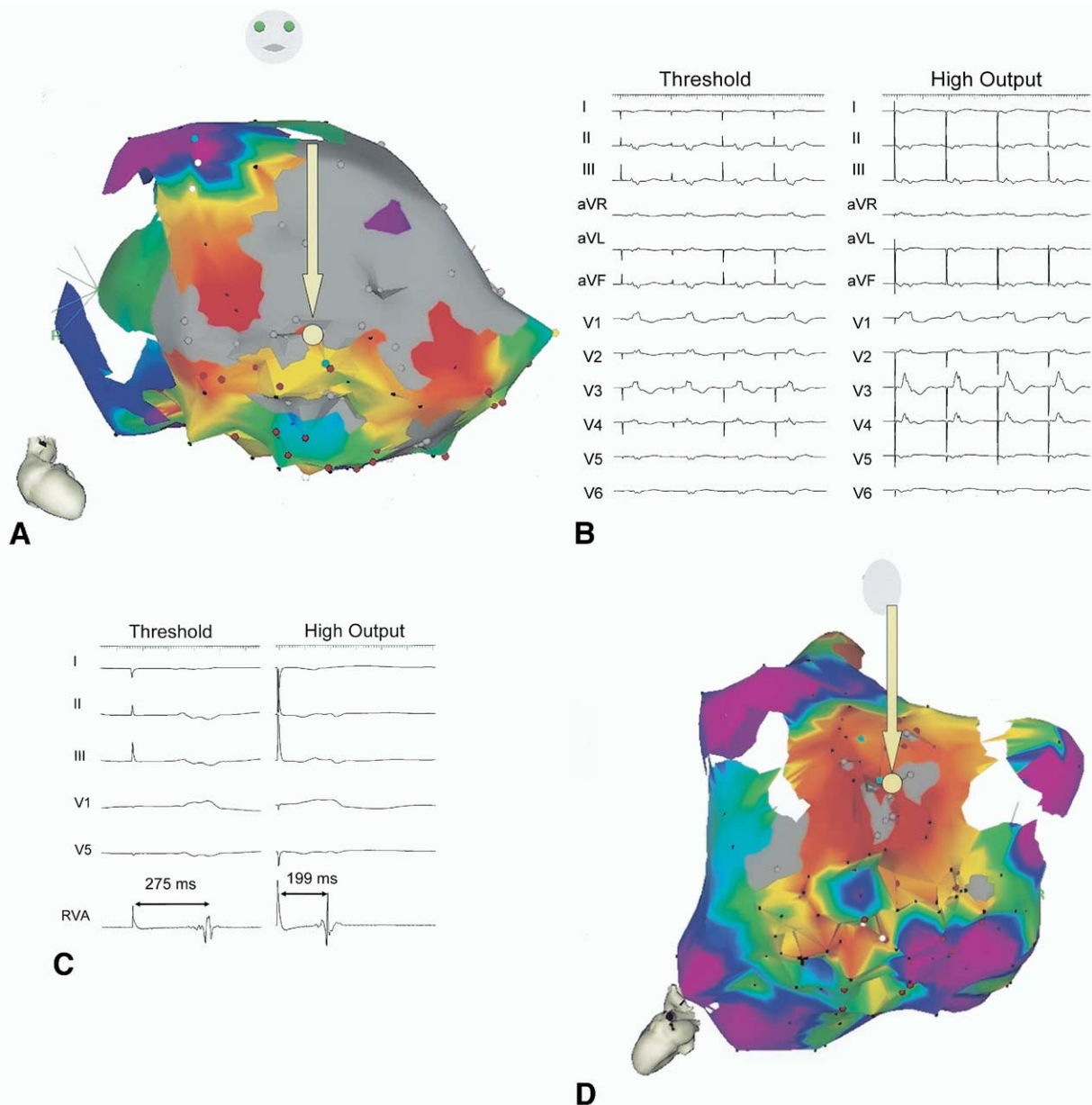
Figure 1. **(A)** Endocardial bipolar electroanatomic map of the left ventricle (LV). Normal voltage areas are **purple**, and electrogram amplitude progressively diminishes as colors proceed to **blue**, **green**, **yellow**, and **red**. Unexcitable scar with pacing threshold >10 mA is **gray** (4). There is a large anteroapical scar **(gray)**. The **yellow arrow and dot** indicate the site of pacing near the apex. **(B)** Paced 12-lead electrocardiograms during threshold **(left)** and 10 mA high-output pacing **(right)** at the site indicated in **panel A**. The initial R-wave in V_3 and V_4 increases with high output pacing. **(C)** Corresponding intracardiac signals from the right ventricle apex (RVA) and five electrocardiogram (ECG) leads. Threshold pacing is shown on the **left**; high-output pacing, on the **right**. The stimulus to RVA electrogram time shortens from 275 to 199 ms with increase in stimulus strength. **(D)** Epicardial bipolar electroanatomic map of the LV. The **yellow arrow and dot** indicate the pacing site at the basal free wall of the LV, between two small areas of unexcitable scar **(gray)**. *Continued on next page.*

precordial transition change of more than one lead; >30° change in QRS axis (6).

Ventricular activation indices were analyzed at threshold and at 10 mA of current output. Comparisons of continuous, paired data were made using paired *t* tests. Where appropriate, results were adjusted using repeated measures analysis of variance to account for multiple observations in individual patients. A p value of <0.05 was considered significant. Analysis was conducted using SAS software (Version 8.2, SAS Institute Inc., Cary, North Carolina).

Electroanatomic LV endocardial voltage maps were analyzed in 10 patients with ventricular dysfunction. One patient had an

additional epicardial map. The mean ejection fraction was 25 ± 9%, mean QRS duration was 151 ± 37 ms, and 80% had coronary artery disease.

Pacing was performed at 95 LV sites (Table 1). Increasing SS from threshold (3.31 ± 1.5 mA) to 10 mA reduced QRS latency (47 ± 52 ms to 32 ± 34 ms; p < 0.001) and conduction time from LV pacing site to RV apex (118 ± 62 ms to 95 ± 43 ms; p < 0.0001).

At 17 of 95 (18%) LV sites in 6 of 10 patients, a significant change in paced QRS morphology was observed. The QRS morphology changes (Fig. 1) were associated with decreases in
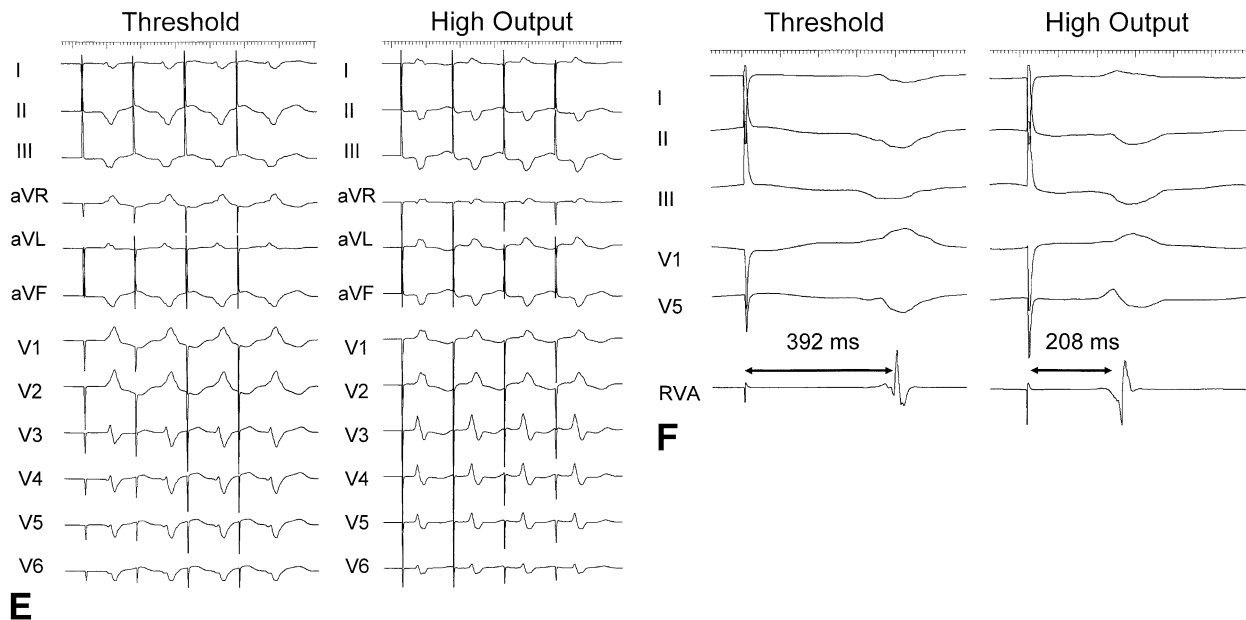
Figure 1 Continued. **(E)** 12-lead ECGs during pacing at threshold **(left)** and 20 mA high-output pacing **(right)** at the site shown in **panel A**. In leads V_3 through V_6, an increase in R-wave occurs with high-output pacing. **(F)** Intracardiac signal from the RVA and five ECG leads. Threshold pacing is shown on the **left**; high output pacing, on the **right**. The stimulus to RVA electrogram time shortens from 392 to 208 ms with increase in stimulus strength.

conduction time to the RV (62 ± 76 ms vs. 14 ± 25 ms at sites with changes; p < 0.0001), QRS latency (45 ± 41 ms vs. 9 ± 26 ms; p < 0.0001), and QRS duration (18 ± 22 ms vs. 4 ± 19 ms; p = 0.03). All ventricles had abnormal low amplitude (<1.5 mV) areas. Pacing sites exhibiting QRS morphology changes with increasing SS had a lower mean electrogram amplitude of 0.8 ± 1.1 mV, compared with sites where SS did not influence QRS morphology (2.3 ± 2.1 mV; p = 0.007).

Surface QRS morphology changes identified pacing sites where VA parameters can be significantly altered with increasing SS, likely reflecting the proximity of pacing sites to discrete areas of conduction block, a more probable scenario in low-voltage areas.

Increasing SS during LV pacing reduces conduction time from the LV to the RV and can produce a sufficient change in VA to produce a change in QRS morphology. These findings are consistent with an increase in virtual electrode size as SS is increased. The effect appears most marked in low-amplitude regions, such as infarct borders (5). Although QRS duration and magnitude of reduction in QRS duration may not reliably correlate with response to CRT (7), VA change is necessary for successful resynchronization. Anatomic constraints in lead position may result in failure to respond to CRT (3). Our findings indicate that SS can be manipulated to influence VA. Potentially, resultant changes in QRS latency and morphology could be used to influence paced interventricular and intraventricular delays during CRT.

Potential limitations of application to CRT include phrenic nerve capture at high SS and shortened device battery life. Study limitations include a small patient number and a potential selection bias of electroanatomic mapping points during ablation. Pacing was endocardial in all but one patient, but epicardial pacing in one patient demonstrated similar VA parameter decreases with QRS morphology changes at three of eight pacing sites. We used unipolar pacing with an anode in the IVC to eliminate the confounding effects of anodal capture, whereas the anode in CRT devices is at the ring of the RV apical lead. The impact of SS when using current CRT systems requires further investigation with hemodynamic correlation.

Increases in SS can change paced VA. The changes can be marked and are more likely to occur in abnormal areas associated with scar or infarction that are marked by low electrogram voltage. Manipulation of the virtual electrode by altering SS may provide a simple means of adjusting CRT.

Usha Tedrow, MD
William H. Maisel, MD, MPH
Laurence M. Epstein, MD
Kyoko Soejima, MD
***William G. Stevenson, MD**

*Brigham and Women's Hospital
Cardiovascular Division, Tower 3-B
75 Francis Street
Boston, MA 02115
E-mail: wstevenson@partners.org

REFERENCES

1. Abraham WT, Fisher WG, Smith AL, et al. Cardiac resynchronization in chronic heart failure. N Engl J Med 2002;346:1845–53.
2. Bradley DJ, Bradley EA, Baughman KL, et al. Cardiac resynchronization and death from progressive heart failure: a meta-analysis of randomized controlled trials. JAMA 2003;289:730–40.
3. St. John Sutton MG, Plappert T, Abraham WT, et al. Effect of cardiac resynchronization therapy on left ventricular size and function in chronic heart failure. Circulation 2003;107:1985–90.
4. Soejima K, Stevenson WG, Maisel WH, et al. Electrically unexcitable scar mapping based on pacing threshold for identification of the reentry circuit isthmus: feasibility for guiding ventricular tachycardia ablation. Circulation 2002;106:1678–83.

5. Marchlinski FE, Callans DJ, Gottlieb CD, et al. Linear ablation lesions for control of unmappable ventricular tachycardia in patients with ischemic and nonischemic cardiomyopathy. Circulation 2000;101:1288–96.
6. Josephson ME, Waxman HL, Cain ME, et al. Ventricular activation during ventricular endocardial pacing. II. Role of pace-mapping to localize origin of ventricular tachycardia. Am J Cardiol 1982;50:11–22.
7. Leclercq C, Faris O, Tunin R, et al. Systolic improvement and mechanical resynchronization does not require electrical synchrony in the dilated failing heart with left bundle-branch block. Circulation 2002;106:1760–3.

Torasemide Inhibits Transcardiac Extraction of Aldosterone in Patients With Congestive Heart Failure

To the Editor: Loop diuretics such as furosemide and torasemide are important for the symptomatic treatment of congestive heart failure (CHF). Recently, in the TOrasemide In Congestive Heart Failure (TORIC) study, torasemide had a more beneficial effect on the mortality and morbidity of patients with CHF than furosemide (1). The mechanism by which torasemide provides a greater benefit than furosemide remains unknown, but experimental studies indicate that torasemide may inhibit the binding of aldosterone (ALD) to its receptor in the cytoplastic fraction of the rat kidney (2,3). Therefore, in the present study, we evaluated the transcardiac extraction of ALD, as a potential marker of ALD action in the heart (4,5), in torasemide therapy compared with furosemide therapy in the treatment of patients with CHF.

The subjects were 60 consecutive patients with CHF (left ventricular ejection fraction <45%). Patients receiving spironolactone were excluded. Informed consent was obtained from all patients before participation in the study, and the protocol was approved by the Human Investigations Committee of our institution. Sixty patients were divided randomly into two groups that were treated with either furosemide (n = 30) or torasemide (n = 30) for one month. In the furosemide group, the same dose of furosemide was continued. In the torasemide group, furosemide was changed to torasemide at a dose with comparable diuretic efficacy (furosemide 40 mg/day changed to torasemide 8 mg/day).

After one month, blood samples for measuring plasma ALD were collected simultaneously from the aortic root (AO) and coronary sinus (CS), and measurements of neurohumoral factors were performed as previously reported (4,5).

All results are expressed as mean values ± SEM. Univariate analyses were performed using the Student t test. Linear regression analysis was used to determine the relationship between continuous variables. A p value < 0.05 was regarded as significant.

There was no difference in patient characteristics between the two groups (Table 1). In the torasemide group, the mean dose of torasemide was 10.1 ± 0.7 mg/day (range, 4 to 16 mg/day).

One month after randomization, there were no differences in hemodynamic parameters. In the furosemide group, the plasma ALD level in the CS was significantly lower than that in the AO (73.1 ± 10.0 pg/ml vs. 56.9 ± 6.5 pg/ml; p < 0.001). In contrast, there was no difference in plasma ALD levels between the AO and the CS in the torasemide group (85.4 ± 10.5 pg/ml vs. 83.1 ± 11.6 pg/ml) (Fig. 1). Plasma procollagen type III aminoterminal peptide in the CS concentration was significantly lower in the torasemide group than that in the furosemide group (0.52 ± 0.03 U/ml vs. 0.67 ± 0.06 U/ml; p < 0.05). There was a significant negative correlation between the dose of torasemide and the transcardiac gradient (AO–CS) of ALD in the torasemide group (r = −0.56, p < 0.01).

We evaluated the transcardiac extraction of ALD as a potential marker of ALD action in the heart (4,5) in patients with CHF. In the furosemide group, the plasma ALD level in the CS was significantly lower than that in the AO. In contrast, there was no difference in plasma ALD level between the AO and the CS in the torasemide group. The transcardiac gradient (AO–CS) of ALD and the extraction ratio of ALD in the AO were significantly lower in the torasemide group than those in the furosemide group. Plasma procollagen type III aminoterminal peptide concentration, a biochemical marker of fibrosis, was significantly lower in the torasemide group than in the furosemide group. These findings may indicate that unlike furosemide, torasemide has an ALD receptor antagonist in the heart. Experimental studies indicate that torasemide inhibits the binding of ALD to its receptor in the cytoplastic fraction of rat kidney (2,3). Moreover, the serum potassium level was significantly higher in the torasemide group than in the furosemide group in a large series (i.e., TORIC study).

Table 1. Clinical Characteristics of Patients in the Furosemide and Torasemide Groups at Randomization

	Furosemide (n = 30)	Torasemide (n = 30)	p Value
Age (yrs)	63.7 ± 1.8	61.5 ± 2.5	NS
Gender (male/female)	23/7	22/8	NS
Etiology of left ventricular dysfunction			
Dilated cardiomyopathy	19	15	NS
Ischemic cardiomyopathy	11	15	NS
NYHA functional class			
II	17	16	NS
III to IV	13	14	NS
Left ventricular ejection fraction by echocardiography (%)	34.9 ± 1.7	33.5 ± 1.6	NS
Treatment			
Dose of furosemide (mg)	46.7 ± 3.1	50.7 ± 3.5	NS
Digitalis	19	15	NS
ACE inhibitors or ARB	21	22	NS
Beta-blockers	13	14	NS

ACE = angiotensin-converting enzyme; ARB = angiotensin receptor blocker; NS = not significant; NYHA = New York Heart Association.